Manipulating Crystals through Photoexcitation-Induced Molecular Realignment

Shen Shen, [a] Gleb Baryshnikov, [b] Bingbing Yue, [c] Bin Wu, [a] Xuping Li, [d] Man Zhang, [a] Hans Ågren, [e,f] and Liangliang Zhu *[a]

[a] State Key Laboratory of Molecular Engineering of Polymers, Department of Macromolecular Science, Fudan University, Shanghai 200438, China. Email: zhuliangliang@fudan.edu.cn

[b] Division of Theoretical Chemistry and Biology School of Biotechnology, KTH Royal Institute of Technology, SE-10691 Stockholm, Sweden.

[c] College of Science, University of Shanghai for Science and Technology, Shanghai 200093, China.

[d] Key Laboratory of Coal Science and Technology, Ministry of Education and Shanxi Province, Taiyuan University of Technology, Taiyuan 030024, China.

[e] Department of Physics and Astronomy, Uppsala University, Box 516, SE-751 20 Uppsala, Sweden.

[f] Tomsk State University, 36 Lenin Avenue, Tomsk, Russia.

SUPPORTING INFORMATION

Contents

S1. General Experimental Methods

Sodium thiophenolate, perfluorobenzene, 1.3-diphenylisobenzofuran (DPBF) and Platium(II) octaethylporphine (PTOEP) used in the experiment were available from energy chemical and used as received. Unless otherwise noted, all the solvents used in this experiment were purchased from Greagent and used directly. The ^{1}H NMR, ^{13}C NMR and ^{19}F NMR were measured on a Bruker 400L spectrometer in chloroform-d and DMSO-d6 using tetramethylsilane as internal standard. Mass spectra were recorded on a Matrix Assisted Laser Desorption Ionization-Time of Flight/Time of Flight (MALDI-TOF) Mass Spectrometer (5800). Powder X-ray diffraction data were collected using a Bruker D8 ADVANCE. The UV-Vis absorption spectra were recorded on a Perkin-Elmer Lambda 750 spectrophotometer. Photoluminescence (PL) spectra were collected on an Edinburgh FLS-1000 luminescence spectrometer equipped with a xenon lamp. The PL decay spectra were recorded on Edinburgh FLS-1000 luminescence spectrometer equipped with a microsecond flashlamp as the excitation source (frequency = 100 Hz) and EPL-375 nm picosecond pulsed diode laser as the excitation source for microsecond and time correlated single-photon counting (TCSPC) measurements, respectively. The IRF was measured using silica solution as the reference standard. The absolute fluorescence quantum efficiencies were measured on QM40 with an integrating sphere (ϕ 150 mm) from Photo Technology International, Inc. (PTI, USA). Dynamic light scattering (DLS) experiments were carried out with Malvern Instruments Nano-Zeta Potential Analyzer ZS-90. Transmission electron microscopy (TEM) was performed on FEI Tecnai G2 F20 S-TWIN with an accelerating voltage of 200 kV. Single crystal X-ray diffraction signals were collected by a Bruker D8 Venture operating at room temperature, and their structures were resolved and analyzed with the assistance of shelx-2014 software. TG analyses were performed on a Metller TG instrument under a dry nitrogen atmosphere at a heating rate of 20 °C/min. DSC analyses were performed with a TAQ2000 instrument under nitrogen atmosphere at a heating rate of 20 °C/min. Optical fluorescence images were taken by using a Nikon microscope at the excitation of UV (365 nm) light. A relatively large concentration (1 mM) of compound 1 was used for the PL spectral measurements in CAN is because 1) The cultivation of 1-V crystals is based on the recrystallization at high concentration under UV irradiation; 2) When recording the average size of compound 1 in response to UV on and off in the DLS test, a high concentration is to ensure that the observable size is instrument reachable.

S2. Synthesis and Crystal Cultivation

The sodium benzenethiolate (520 mg, 4 mmol) and perfluorobenzene (115 µL, 1 mmol) were dissolved in N,N-Dimethylformamide (20 mL) and refluxed at 40 ^{o}C for 48 h. A precipitate was obtained with the addition of water (20 mL). The resulting precipitate was filtrated and washed with ethanol and water to give yellow powder (**1**-powder) in 76.2 % yield (416.40 mg). The as prepared powder was purified in silica gel column of petroleum ether (PE) and DCM (10:1), then crystallization in ACN and mixed solvent of EtOH and DCM (EtOH:DCM=1:2), respectively. The crystals recrystallized from the ACN and mixed solvent of EtOH and DCM showed blue and yellow fluorescence, as named **1-B** and **1-Y**, respectively. We then employed continuous UV irradiation from a handheld 365 UV lamp (3.70 mW/cm^{2}) for 4 hours during the above two crystallization process before amount crystals deposited in the single neck round bottom flask, yielding a novel violet fluorescence single crystal of 1, i.e. **1-V**. ^{1}H NMR (400 MHz, chloroform-*d*) δ= 7.26-7.16 (m, 20H) ppm. ^{13}C NMR (100 MHz, chloroform-*d*) δ= (160.53, 158.07, d, J = 249), 134.69, 129.47, 129.08, 128.96 (d), 127.01, ppm. MS: MALDI-TOF MS, m/z: calculated for $C_{30}H_{20}F_{2}S_{4}$, 546.04; found m/z, 546.10. The structural characterization is shown in Fig. S4.

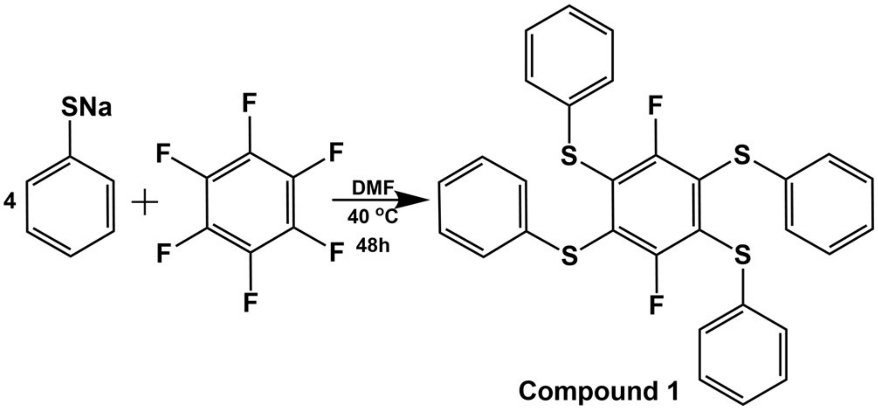

Fig. S1. Synthetic route for Compound **1**.

S3. Computational Details

The molecular structures for the different polymorphs of Compound **1** (marked as **1-Y**, **1-B** and **1-V**) required for the quantum-chemical calculations were initially extracted from the single-crystal X-ray diffraction experiment. All the crystals contain two slightly different conformers in the elementary cell of each **1-Y**, **1-B** and **1-V** polymorph. Upon the optimization procedure both conformers lead to the same global minimum structure independently on the initial structure extracted from **1-Y**, **1-B** or **1-V** elementary cell. Thus, to investigate the photophysical behavior of particular conformers stable only in crystal state we have performed single point B3LYP/6-311++G(d,p) calculations[1] accounting for the empirical dispersion correction (GD3) in order to estimate the relative energy of different conformers. Based on the same geometries we have calculated the energies of the 10 singlet and 10 triplet excited states by the TDDFT method[2] at the cam-B3LYP/TZP level of theory[3]. The SOC matrix elements, (i=1-10; j=1-10) were calculated perturbatively[4] as root mean squares, i.e. as square root of the sum of squares of spin-orbit coupling matrix elements of all triplet state sublevels (m=0,±1) of the uncoupled states:

$$\left\langle \mathrm{S}_i \middle| \hat{\mathrm{H}}_{\mathrm{SO}} \middle| \mathrm{T}_j \right\rangle = \sqrt{\sum_{m=0,\pm1} \left\langle \mathrm{S}_i \middle| \hat{\mathrm{H}}_{\mathrm{SO}} \middle| \mathrm{T}_j^m \right\rangle^2} \quad (1)$$

The spin-orbit coupling operator was considered in our calculations within the zeroth-order regular approximation (ZORA).[5] The cam-B3LYP was used because of the charge-transfer nature of the S_1 and low-lying triplet states, while B3LYP functional strongly underestimates the energy of these states (it was recently shown for the related perchalcogenated (O, S, and Se) arenes).[6] In order to understand the structural changes happened with the 1 molecule upon excitation, we have also optimized its structure in the first excited singlet (S_1) and triplet (T_1) states by the (TD)DFT-B3LYP/6-311++G(d,p) and UB3LYP/6-311++G(d,p) methods, respectively. This type of calculations as well as GD3-B3LYP/6-311++G(d,p) calculations were performed within Gaussian16 software,[7] while the cam-B3LYP/TZP calculations and subsequent SOC calculations have been carried out within ADF2018 package.[8]

S4. Additional Results

Table S1 Crystal data and refinement details for **1-Y**

Compound	**1-Y**	
CCDC number	2080762	
Empirical formula	C30 H20 F2 S4	
Formula weight	546.70	
Temperature	298(2) K	
Wavelength	1.34138 A	
Crystal system, space group	Triclinic, $P\bar{1}$	
Unit cell dimensions	a = 9.6192(3) Å	α = 76.315(2)°
	b = 14.1327(5) Å	β= 88.160(2)°
	c = 14.9715(5) Å	γ = 88.8180(10)°
Volume	1976.33(12) A^3	
Z, Calculated density	3, 1.378 g/cm^3	
Absorption coefficient	2.359 mm^-1	
F(000)	846	
Crystal size	0.032 x 0.025 x 0.022 mm^3	
Theta range for data collection	4.735 to 54.879°	
Limiting indices	-11<=h<=11, -17<=k<=17, -18<=l<=17	
Reflections collected / unique	24199 / 7435 [R(int) = 0.0485]	
Completeness to theta = 53.594	99.3 %	
Absorption correction	Semi-empirical from equivalents	
Max. and min. transmission	0.751 and 0.527	
Refinement method	Full-matrix least-squares on F^2	
Data / restraints / parameters	7435 / 0 / 488	
Goodness-of-fit on F^2	1.030	
Final R indices [I>2sigma(I)]	R1 = 0.0377, wR2 = 0.1003	
R indices (all data)	R1 = 0.0454, wR2 = 0.1058	
Largest diff. peak and hole	0.337 and -0.355 e.A^-3	

Table S2 Crystal data and refinement details for **1-B**

Compound	**1-B**	
CCDC number	2080763	
Empirical formula	C30 H20 F2 S4	
Formula weight	546.70	
Temperature	298(2) K	
Wavelength	1.34138 A	
Crystal system, space group	Triclinic, $P\overline{1}$	
Unit cell dimensions	a = 9.6203(3) Å	α = 76.2930(10)°
	b = 14.1325(5) Å	β= 88.135(2)°
	c = 14.9666(5) Å	γ = 88.840(2)°
Volume	1975.68(11) A^3	
Z, Calculated density	3, 1.378 g/cm^3	
Absorption coefficient	2.359 mm^-1	
F(000)	846	
Crystal size	0.270 x 0.090 x 0.030 mm^3	
Theta range for data collection	4.000 to 58.492°	
Limiting indices	-12<=h<=12, -17<=k<=17, -19<=l<=19	
Reflections collected / unique	35784 / 8473 [R(int) = 0.0326]	
Completeness to theta = 53.594	99.7 %	
Absorption correction	Semi-empirical from equivalents	
Max. and min. transmission	0.752 and 0.577	
Refinement method	Full-matrix least-squares on F^2	
Data / restraints / parameters	8473 / 0 / 487	
Goodness-of-fit on F^2	1.044	
Final R indices [I>2sigma(I)]	R1 = 0.0316, wR2 = 0.0857	
R indices (all data)	R1 = 0.0356, wR2 = 0.0889	
Largest diff. peak and hole	0.251 and -0.273 e.A^-3	

Table S3 Crystal data and refinement details for **1-V**

Compound	**1-V**	
CCDC number	2080761	
Empirical formula	C30 H20 F2 S4	
Formula weight	546.70	
Temperature	298(2) K	
Wavelength	1.34138 A	
Crystal system, space group	Triclinic, $P\bar{1}$	
Unit cell dimensions	a = 9.6172(2)Å	α = 76.3000(10)^{o}
	b = 14.1315(3) Å	β= 88.1760(10)^{o}
	c = 14.9727(3) Å	γ = 88.8440(10)^{o}
Volume	1975.81(7)A^3	
Z, Calculated density	3, 1.378 g/cm^3	
Absorption coefficient	2.359 mm^-1	
F(000)	846	
Crystal size	0.056 x 0.047 x 0.035 mm^3	
Theta range for data collection	4.856 to 54.892^{o}	
Limiting indices	-10<=h<=11, -17<=k<=17, -18<=l<=18	
Reflections collected / unique	25354 / 77432 [R(int) = 0.0283]	
Completeness to theta = 53.594	99.2 %	
Absorption correction	Semi-empirical from equivalents	
Max. and min. transmission	0.751 and 0.590	
Refinement method	Full-matrix least-squares on F^2	
Data / restraints / parameters	7432 / 0 / 488	
Goodness-of-fit on F^2	1.024	
Final R indices [I>2sigma(I)]	R1 = 0.0304, wR2 = 0.0808	
R indices (all data)	R1 = 0.0341, wR2 = 0.0838	
Largest diff. peak and hole	0.193 and -0.231e.A^-3	

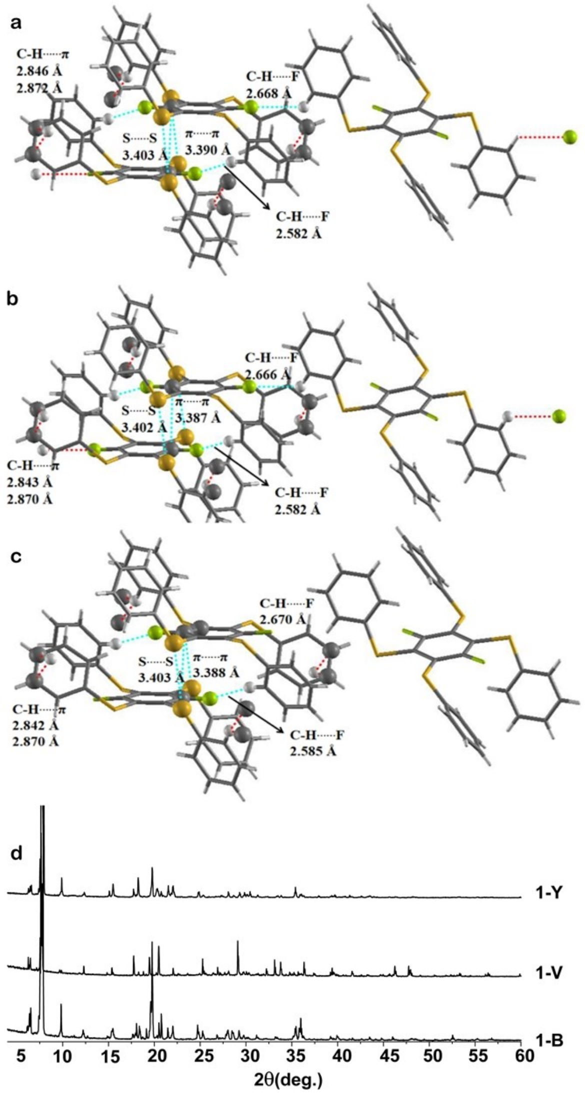

Fig. S2. Intermolecular short interaction displays of (a) **1-Y** (b) **1-B** (c) **1-V** and (d) its corresponding powder X-ray diffraction spectra.

Table S4. 4.1 Selected torsion angles (θ, deg.) for the different conformers of **1**

Molecule	θ_1/ θ_2 [A]	θ_1/ θ_2 [B]	θ_1/ θ_2 [C]	θ_1/ θ_2 [D]	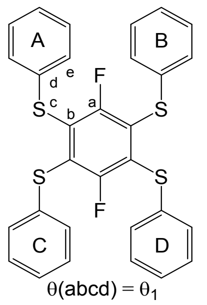 θ(abcd) = θ_1 θ(bcde) = θ_2
1-Y (I)	-62.5/-20.4	61.5/26.7	-53.5/-30.6	41.5/48.7	
1-Y (II)	-50.6/-24.1	58.1/38.6	-58.1/-38.6	50.6/24.1	
1-B (I)	-62.2/-20.5	61.6/26.5	-53.6/-30.5	41.6/48.6	
1-B (II)	-50.4/-23.9	57.8/38.8	-57.8/-38.8	50.4/23.9	
1-V (I)	-62.3/-20.5	61.5/26.5	-53.6/-30.5	41.6/48.8	
1-V (II)	-50.5/-24.1	58.0/38.8	-58.0/-38.8	50.5/24.1	
1-opt (S_0)	-56.2/-53.8	55.5/53.0	-55.5/-53.0	56.2/53.8	
1-opt (S_1)	-87.0/-0.1	96.0/2.5	-87.0/-0.1	96.0/2.5	
1-opt (T_1)	-51.8/-44.0	52.2/37.0	-51.8/-44.0	52.2/37.0	

4.2 Selected bond lengths for the different conformers of **1**

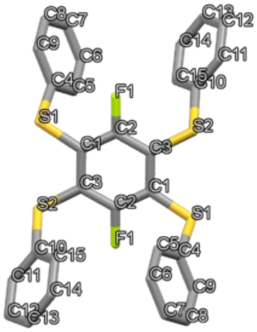

1-Y Symmetrical II

C-S bond (Å)		C-C central core (Å)		C-F bond (Å)
C4-S1	1.774	C1-C3	1.409	1.353
C1-S1	1.764	C3-C2	1.381	
C10-S2	1.773	C2-C1	1.386	
C3-S2	1.761			

1-B Symmetrical II

C-S bond (Å)		C-C central core (Å)		C-F bond (Å)
C4-S1	1.771	C1-C3	1.404	1.344
C1-S1	1.763	C3-C2	1.388	
C10-S2	1.775	C2-C1	1.384	
C3-S2	1.765			

1-V Symmetrical II

C-S bond (Å)		C-C central core (Å)		C-F bond (Å)
C4-S1	1.776	C1-C3	1.407	1.346
C1-S1	1.767	C3-C2	1.385	
C10-S2	1.772	C2-C1	1.384	
C3-S2	1.762			

S_0 Symmetrical II

C-S bond (Å)		C-C central core (Å)		C-F bond (Å)
C4-S1	1.798	C1-C3	1.411	1.343
C1-S1	1.790	C3-C2	1.396	
C10-S2	1.798	C2-C1	1.396	
C3-S2	1.790			

S_1 Symmetrical II

C-S bond (Å)		C-C central core (Å)		C-F bond (Å)
C4-S1	1.798	C1-C3	1.469	1.350
C1-S1	1.768	C3-C2	1.393	
C10-S2	1.781	C2-C1	1.390	
C3-S2	1.761			

T_1 Symmetrical II

C-S bond (Å)		C-C central core (Å)		C-F bond (Å)
C4-S1	1.799	C1-C3	1.483	1.353
C1-S1	1.763	C3-C2	1.386	
C10-S2	1.790	C2-C1	1.393	
C3-S2	1.763			

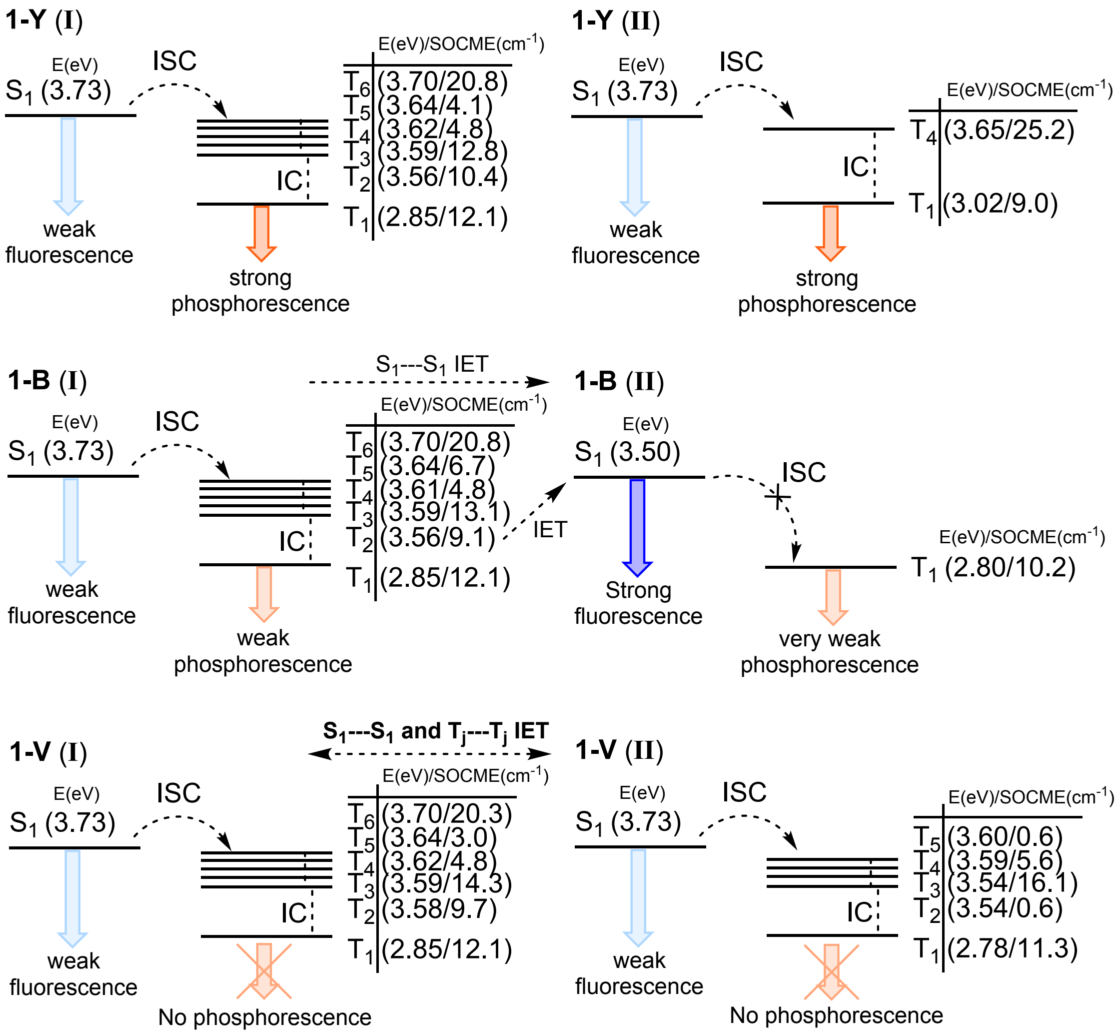

Fig. S3. The general mechanism of conformation-dependent emission for **1-Y**, **1-B**, and **1-V**. Abbreviations ISC, IC, IET and SOCME correspond to the intersystem-crossing, internal conversion, intermolecular energy transfer and spin-orbit coupling matrix elements, respectively.

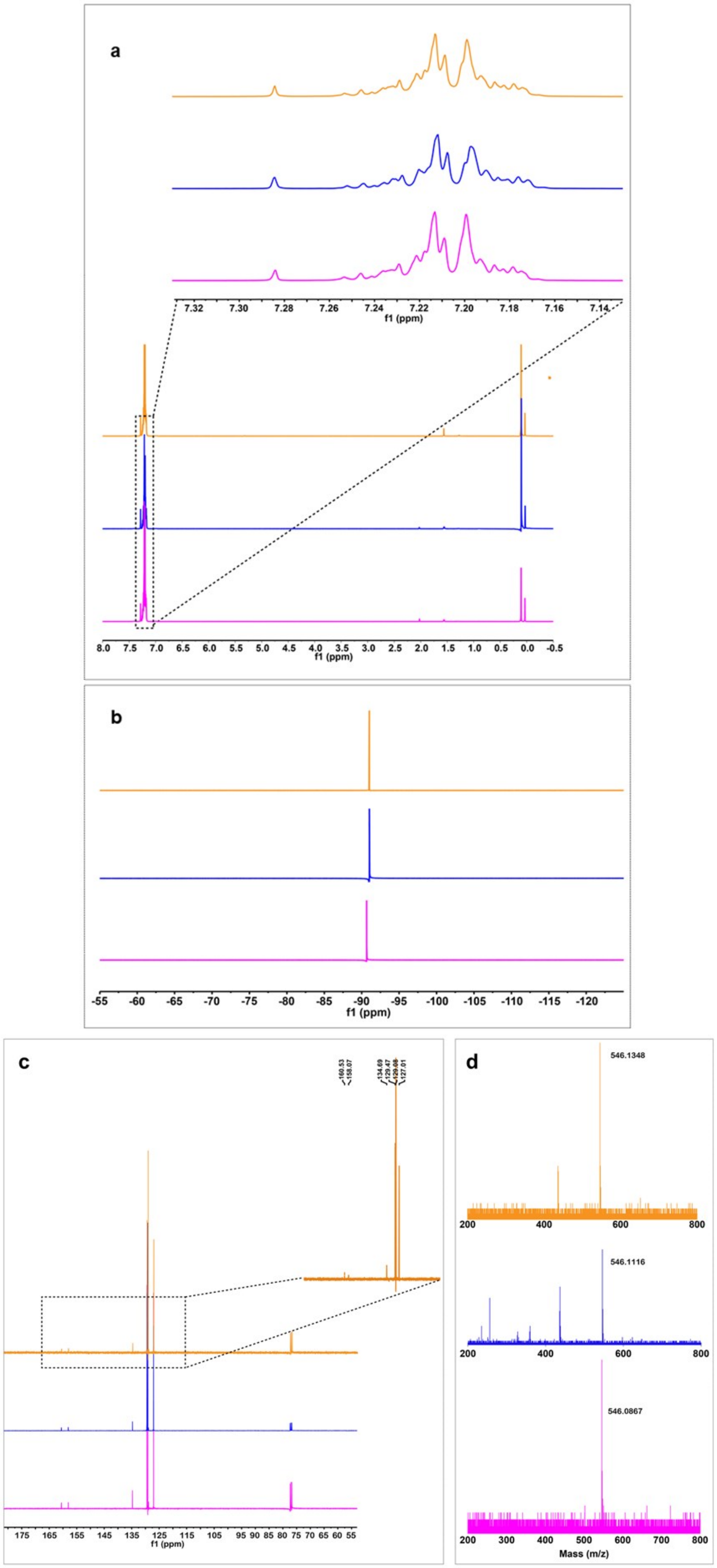

Fig. S4. (a) ^{1}H NMR, (b) ^{19}F NMR, (c) ^{13}C NMR spectra of **1-Y** (yellow line), **1-B** (blue line), **1-V** (violet line) in chloroform-*d*, and (d) MALDI-TOF mass spectra of **1-Y** (yellow line), **1-B** (blue line), **1-V** (violet line).

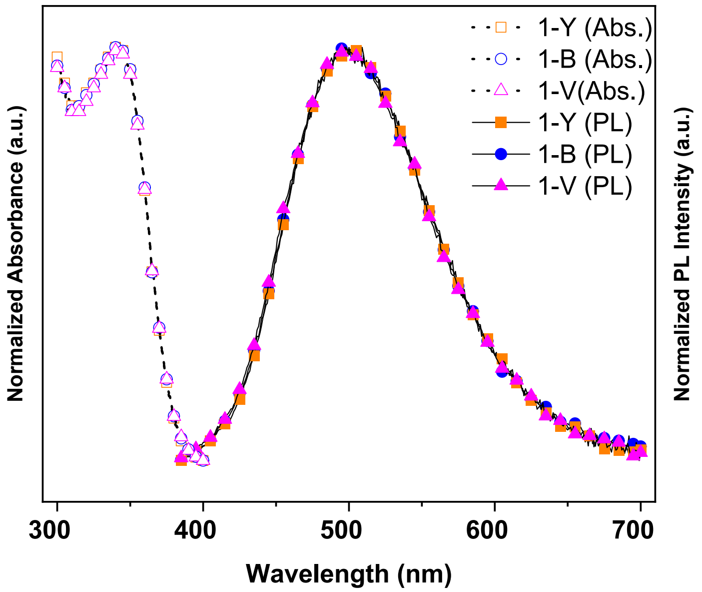

Fig. S5. Normalized absorption (Abs.) spectra and photoluminescence (PL) spectra of **1-Y**, **1-B** and **1-V** in ACN (1 mM).

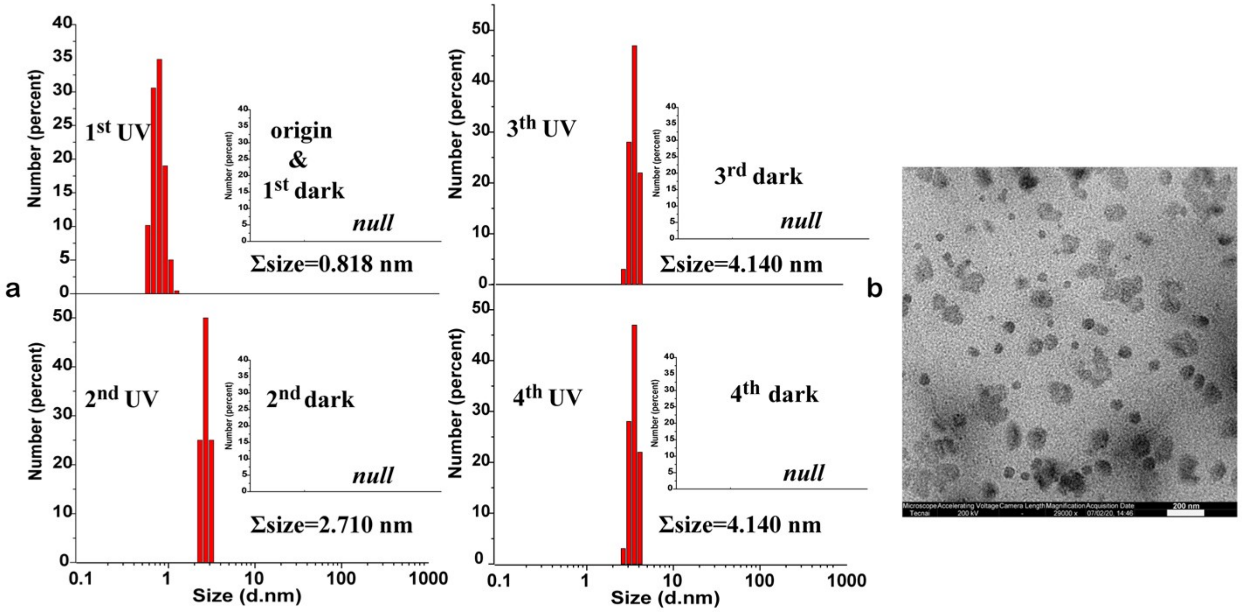

Fig. S6. (a) DLS results of Compound **1** in ACN (1mM) in four cycles of UV irradiation (a handheld lamp, 3.70mW/cm^2) for 1 min and then placed in a dark state for 15 min. (b) TEM images of 1 in ACN after photoirradiation for 1min.

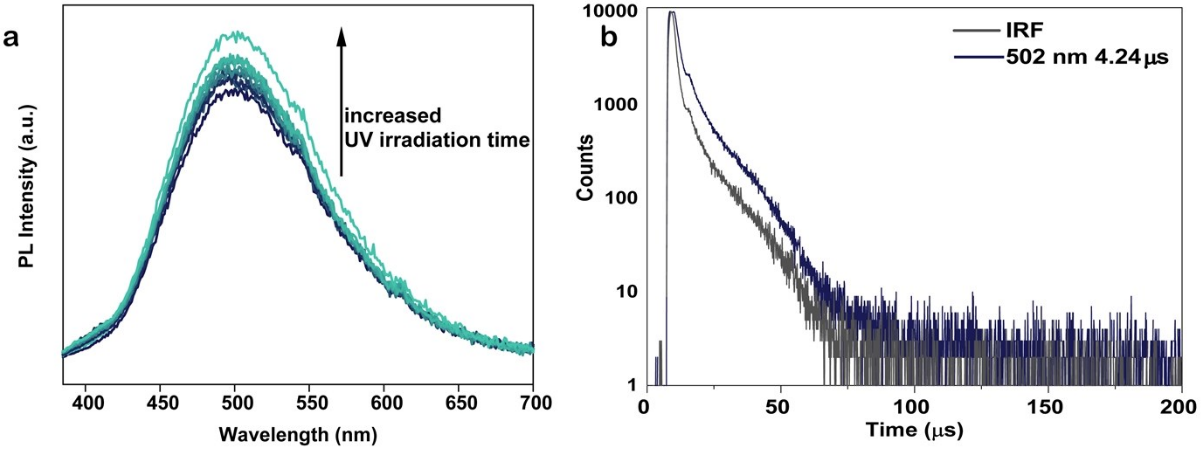

Fig. S7. (a) PL spectra of Compound **1** in ACN at room temperature (1 mM) with increased UV (365 nm) irradiation time. (b) PL decay curves of Compound **1** in ACN (1mM) at room temperature.

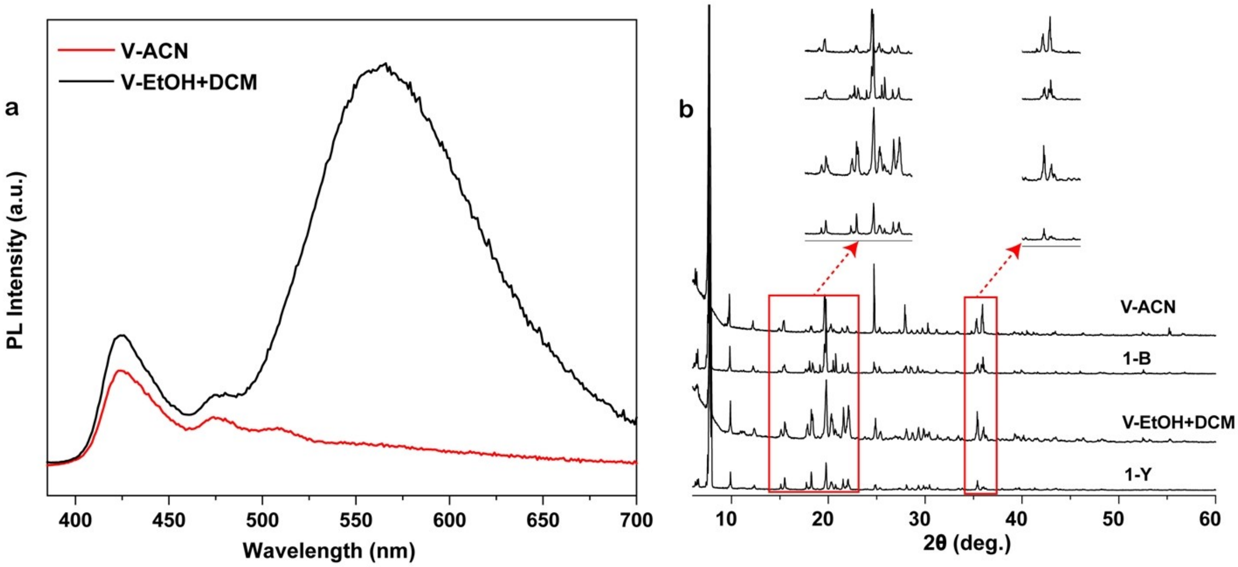

Fig. S8. (a) PL spectra and (b) Powder X-ray diffraction of **1-V** recrystallized in ACN (V-ACN) and in mixed solvent of EtOH and DCM (V-EtOH+DCM).

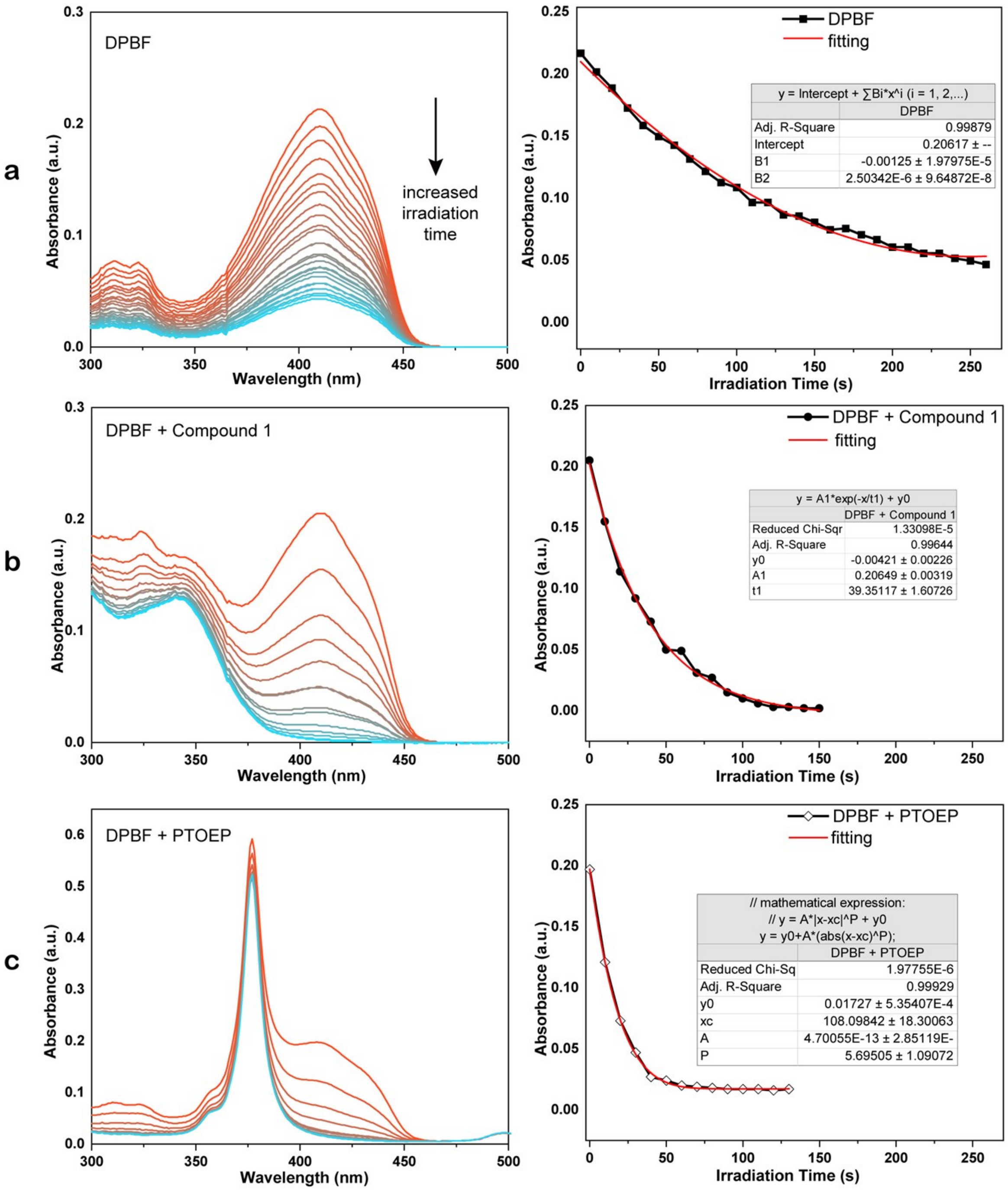

y = Intercept + ∑Bi*x^i (i = 1, 2,...)	
	DPBF
Adj. R-Square	0.99879
Intercept	0.20617 ± --
B1	-0.00125 ± 1.97975E-5
B2	2.50342E-6 ± 9.64872E-8

y = A1*exp(-x/t1) + y0	
	DPBF + Compound 1
Reduced Chi-Sqr	1.33098E-5
Adj. R-Square	0.99644
y0	-0.00421 ± 0.00226
A1	0.20649 ± 0.00319
t1	39.35117 ± 1.60726

// mathematical expression:
// y = A*|x-xc|^P + y0
y = y0+A*(abs(x-xc)^P);	

	DPBF + PTOEP
Reduced Chi-Sq	1.97755E-6
Adj. R-Square	0.99929
y0	0.01727 ± 5.35407E-4
xc	108.09842 ± 18.30063
A	4.70055E-13 ± 2.85119E-
P	5.69505 ± 1.09072

Fig. S9. UV-vis absorption spectra after irradiation at 365 nm for different times (left) and the absorption intensity of DPBF at 410 nm versus the UV irradiation time (right) of (a) DPBF (10 µM), (b) DPBF with Compound **1** (10 µM), (d) DPBF with PTOEP (10 µM).

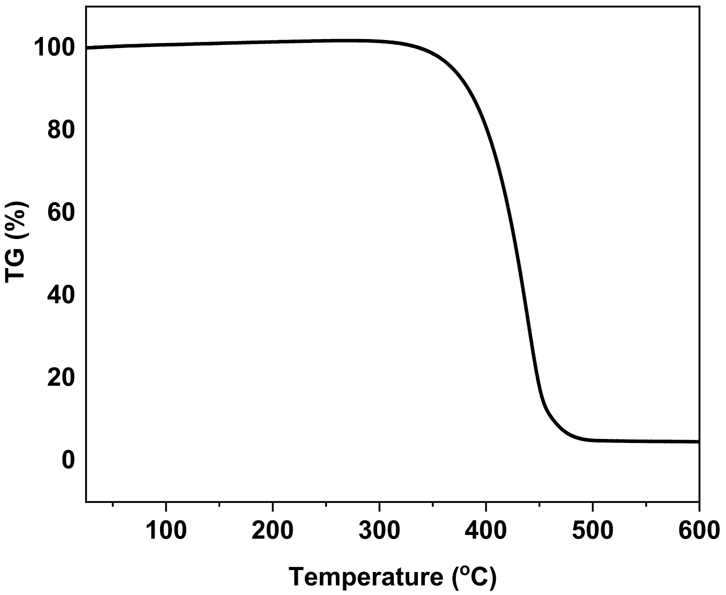

Fig. S10. Thermogravimetric analysis of **1**-powder.

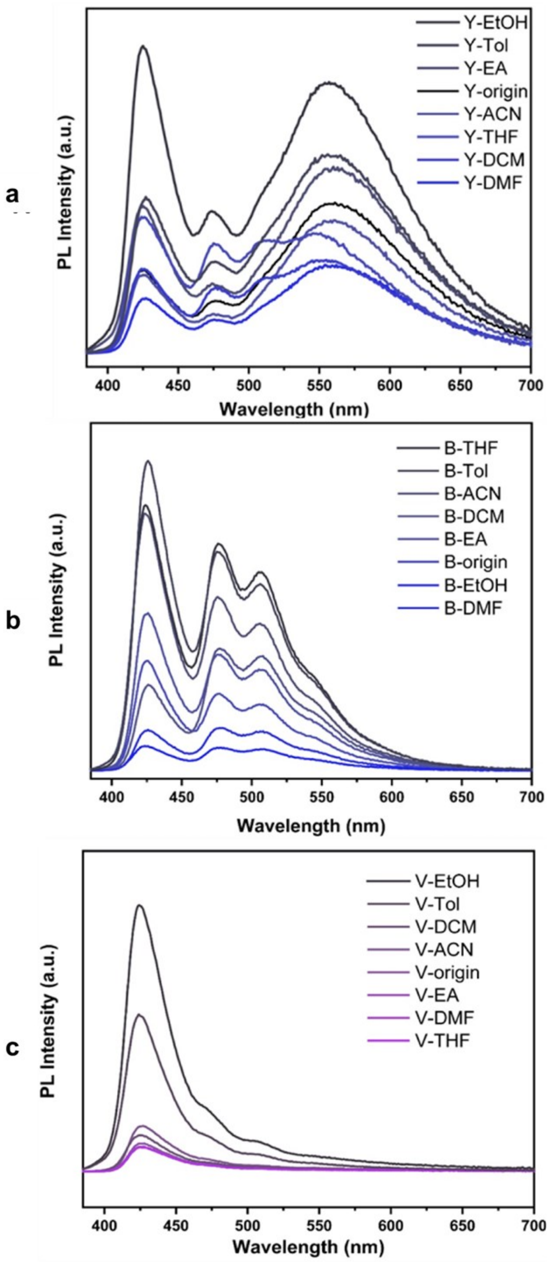

Fig. S11. PL spectra of (a) **1-Y**, (b) **1-B**, (c) **1-V** crystals fumed with ethanol (EtOH), toluene (Tol), dichloromethane (DCM), acetonitrile (ACN), ethyl acetate (EA), N,N-dimethylformamide (DMF) and tetrahydrofuran (THF) for 5 min.

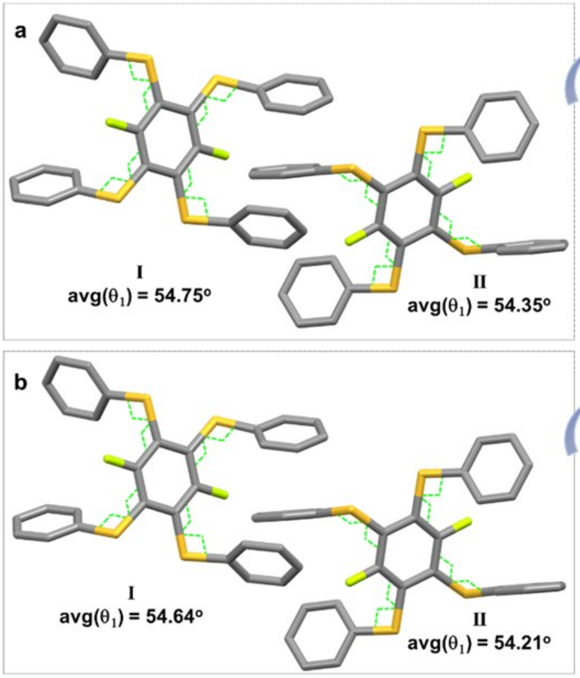

1-Y Symmetrical II

C-S bond (Å)		C-C central core (Å)		C-F bond (Å)
C4-S1	1.774	C1-C3	1.409	1.353
C1-S1	1.764	C3-C2	1.381	
C10-S2	1.773	C2-C1	1.386	
C3-S2	1.761			

1-Y-UV 5min Symmetrical II

C-S bond (Å)		C-C central core (Å)		C-F bond (Å)
C4-S1	1.770	C1-C3	1.405	1.349
C1-S1	1.763	C3-C2	1.389	
C10-S2	1.774	C2-C1	1.380	
C10-S2	1.767			

Fig. S12. The unit cell displays and representative average torsion angles and bond lengths of the SCs. (a) **1-Y**. (b) **1-Y** after an *in situ* UV irradiation for 5 min (**1-Y-UV 5min**).

Table S5. Crystal data and refinement details for **1-Y-UV 5min**

Compound	**1-Y-UV 5min**	
CCDC number	2080764	
Empirical formula	C30 H20 F2 S4	
Formula weight	546.70	
Temperature	298(2) K	
Wavelength	1.34138 A	
Crystal system, space group	Triclinic, $P\bar{1}$	
Unit cell dimensions	a = 9.6194(2) Å	α = 76.2900(10)°
	b = 14.1326(3) Å	β= 88.1700(10)°
	c = 14.9765(3) Å	γ = 88.8540(10)°
Volume	1976.83(7)A^3	
Z, Calculated density	3, 1.378 g/cm^3	
Absorption coefficient	2.358 mm^-1	
F(000)	846	
Crystal size	0.032 x 0.025 x 0.022 mm^3	
Theta range for data collection	4.000 to 54.867°	
Limiting indices	-11<=h<=11, -17<=k<=17, -18<=l<=17	
Reflections collected / unique	25912 / 7450 [R(int) = 0.0514]	
Completeness to theta = 53.594	99.4 %	
Absorption correction	Semi-empirical from equivalents	
Max. and min. transmission	0.751 and 0.483	
Refinement method	Full-matrix least-squares on F^2	
Data / restraints / parameters	7450 / 0 / 488	
Goodness-of-fit on F^2	1.042	
Final R indices [I>2sigma(I)]	R1 = 0.0382, wR2 = 0.1023	
R indices (all data)	R1 = 0.0419, wR2 = 0.1058	
Largest diff. peak and hole	0.377 and -0.327 e.A^-3	

S5. References

[1] (a) A. D. Becke, J. *Chem. Phys.,* 1993, **98**, 5648-5652; (b) C. Lee, W. Yang and R. G. Parr, *Phy. Rev. B,* 1988, **37**, 785-789; (c) A. D. McLean and G. S. Chandler, *J. Chem. Phys.,* 1980, **72**, 5639-5648; (d) R. Krishnan, J. S. Binkley, R. Seeger and J. A. Pople, *J. Chem. Phys.,* 1980, **72**, 650-654; (e) R. C. Binning Jr. and L. A. Curtiss, *J. Comput. Chem.,* 1990, **11**, 1206-1216.

[2] R. Bauernschmitt and R. Ahlrichs, *Chem. Phys. Lett.,* 1996, **256**, 454-464.

[3] (a) T. Yanai, D. P. Tew and N. C. Handy, *Chem. Phys. Lett.,* 2004, **393**, 51-57; (b) E. Van Lenthe and E. J. Baerends, *J. Comput. Chem.,* 2003, **24**, 1142-1156.

[4] F. Wang and T. Ziegler, *J. Chem. Phys.,* 2005, **123**, 154102.

[5] (a) E. van Lenthe, J. G. Snijders and E. J. Baerends, *J. Chem. Phys.,* 1996, **105**, 6505-6516; (b) E. v. Lenthe, E. J. Baerends and J. G. Snijders, *J. Chem. Phys.,* 1993, **99**, 4597-4610.

[6] T. Weng, G. Baryshnikov, C. Deng, X. Li, B. Wu, H. Wu, H. Ågren, Q. Zou, T. Zeng and L. Zhu, *Small,* 2020, **16**, 1906475.

[7] Gaussian 16, Revision C.01, M. J. Frisch, G. W. Trucks, H. B. Schlegel, G. E. Scuseria, M. A. Robb, J. R. Cheeseman, G. Scalmani, V. Barone, G. A. Petersson, H. Nakatsuji, X. Li, M. Caricato, A. V. Marenich, J. Bloino, B. G. Janesko, R. Gomperts, B. Mennucci, H. P. Hratchian, J. V. Ortiz, A. F. Izmaylov, J. L. Sonnenberg, D. Williams-Young, F. Ding, F. Lipparini, F. Egidi, J. Goings, B. Peng, A. Petrone, T. Henderson, D. Ranasinghe, V. G. Zakrzewski, J. Gao, N. Rega, G. Zheng, W. Liang, M. Hada, M. Ehara, K. Toyota, R. Fukuda, J. Hasegawa, M. Ishida, T. Nakajima, Y. Honda, O. Kitao, H. Nakai, T. Vreven, K. Throssell, J. A. Montgomery, Jr., J. E. Peralta, F. Ogliaro, M. J. Bearpark, J. J. Heyd, E. N. Brothers, K. N. Kudin, V. N. Staroverov, T. A. Keith, R. Kobayashi, J. Normand, K. Raghavachari, A. P. Rendell, J. C. Burant, S. S. Iyengar, J. Tomasi, M. Cossi, J. M. Millam, M. Klene, C. Adamo, R. Cammi, J. W. Ochterski, R. L. Martin, K. Morokuma, O. Farkas, J. B. Foresman, and D. J. Fox, Gaussian, Inc., Wallingford CT, 2016.

[8] G.te Velde, F.M. Bickelhaupt, E.J. Baerends, C. Fonseca Guerra, S.J.A. van Gisbergen, J.G. Snijders and T. Ziegler, *J. Comput. Chem.,* 2001, **22**, 931.